Color Vision in Aniridia

Hilde R. Pedersen,[1] Lene A. Hagen,[1] Erlend C. S. Landsend,[2] Stuart J. Gilson,[1] Øygunn A. Utheim,[2,3] Tor P. Utheim,[1–4] Maureen Neitz,[5] and Rigmor C. Baraas[1]

[1]National Centre for Optics, Vision and Eye Care, Faculty of Health and Social Sciences, University College of Southeast Norway, Kongsberg, Norway
[2]Department of Ophthalmology, Oslo University Hospital, Oslo, Norway
[3]Department of Medical Biochemistry, Oslo University Hospital, Oslo, Norway
[4]Department of Ophthalmology, Drammen Hospital, Drammen, Norway
[5]Department of Ophthalmology, University of Washington, Seattle, Washington, United States

Correspondence: Rigmor C. Baraas, National Centre for Optics, Vision and Eye Care, Faculty of Health and Social Sciences, University College of Southeast Norway, Kongsberg, Norway;
rigmor.baraas@usn.no.

Submitted: September 25, 2017
Accepted: March 27, 2018

Citation: Pedersen HR, Hagen LA, Landsend ECS, et al. Color vision in aniridia. *Invest Ophthalmol Vis Sci*. 2018;59:2142–2152. https://doi.org/10.1167/iovs.17-23047

Purpose. To assess color vision and its association with retinal structure in persons with congenital aniridia.

Methods. We included 36 persons with congenital aniridia (10–66 years), and 52 healthy, normal trichromatic controls (10–74 years) in the study. Color vision was assessed with Hardy-Rand-Rittler (HRR) pseudo-isochromatic plates (4th ed., 2002); Cambridge Color Test and a low-vision version of the Color Assessment and Diagnosis test (CAD-LV). Cone-opsin genes were analyzed to confirm normal versus congenital color vision deficiencies. Visual acuity and ocular media opacities were assessed. The central 30° of both eyes were imaged with the Heidelberg Spectralis OCT2 to grade the severity of foveal hypoplasia (FH, normal to complete: 0–4).

Results. Five participants with aniridia had cone opsin genes conferring deutan color vision deficiency and were excluded from further analysis. Of the 31 with aniridia and normal opsin genes, 11 made two or more red-green (RG) errors on HRR, four of whom also made yellow-blue (YB) errors; one made YB errors only. A total of 19 participants had higher CAD-LV RG thresholds, of which eight also had higher CAD-LV YB thresholds, than normal controls. In aniridia, the thresholds were higher along the RG than the YB axis, and those with a complete FH had significantly higher RG thresholds than those with mild FH ($P = 0.038$). Additional increase in YB threshold was associated with secondary ocular pathology.

Conclusions. Arrested foveal formation and associated alterations in retinal processing are likely to be the primary reason for impaired red-green color vision in aniridia.

Keywords: aniridia, color vision, foveal hypoplasia, retinal development

The reported prevalence of congenital aniridia in Norway and Sweden is about 1:72,000.[1] Characteristic features in aniridia include absence or hypoplasia of the iris, foveal hypoplasia (FH) and nystagmus, while optic nerve hypoplasia (ONH) occurs but is less common.[2,3] Aniridia may lead to severe visual impairment, although there is considerable phenotypic variation between and within families.[4,5] Secondary progressive ocular complications, such as aniridia associated keratopathy (AAK), cataract, and glaucoma, are common from adolescence and onward.[4,6,7]

Aniridia-like phenotypes may be caused by mutations in genes such as *FOXC1* and *PITX2*,[8] but typically (>85%) it is caused by loss of one functional copy of the *PAX6* gene,[9] with about one-third of cases being sporadic and two-thirds being inherited as an autosomal-dominant trait.[10] The *PAX6* gene is located on chromosome band 11p13 and regulates transcription of other genes important for ocular development. Gene dysfunction may affect multiple ocular structures.[11] Aniridia phenotypes caused by *PAX6* mutations are associated with different degrees of foveal hypoplasia, most commonly to a degree of no foveal avascular zone (FAZ) and no foveal depression.[12,13] It is known that *Pax6* acts on several target genes required for retinal ganglion cell development and retina neurogenesis.[14,15] *PAX6/Pax6* dosage expression varies during normal development,[16–18] and animal studies show that abnormal *PAX6/Pax6* expression affects the distribution, development, and the balance of different types of retinal cells.[17,19]

Normal foveal development depends on a high ganglion cell count within the central retina[20] and is characterized by formation of a FAZ before the foveal depression is formed, displacement of the inner retinal layers and postnatal elongation and migration of cones toward the center of the fovea.[21–23] Trichromatic color vision requires a normally developed healthy functioning retina containing cone photoreceptors with three different opsins (L, M, and S cones),[24] including specialized postreceptoral interaction with other retinal neurons (bipolar, amacrine, horizontal, and ganglion cells).[25] During human fetal retinal development, S cones appear earlier than L and M cones,[26] with S cones present around the start of FAZ development and before the foveal depression develops.[27] Disruptions in foveal development that occur around this time may therefore affect L and M cone development, density and its associated retinal circuitry, limiting the number of bipolar and horizontal cell contacts needed for normal red-green vision, more so than for blue-yellow vision. Thus, it is

reasonable to hypothesize that foveal hypoplasia associated with aniridia could affect red-green color discrimination.

Here, results are reported from experiments using computerized color vision tests together with retinal imaging (OCT and color fundus photo) to examine color vision and retinal layer structure in persons with congenital aniridia. These experiments provide insight into the association between the degree of arrested foveal formation in aniridia and impairment of red-green color vision and how this is accompanied by impairment of yellow-blue color vision when secondary pathology is advanced.

Methods

Participants

We recruited 36 participants previously diagnosed with congenital aniridia (15 males), aged between 9 and 72 years, and 52 healthy, normal trichromatic controls (21 males), aged between 10 and 74 years, to the study. Participants with aniridia were recruited through the Norwegian Association of Aniridia, whereas normal controls were recruited through the National Centre for Optics, Vision and Eye Care, University College of Southeast Norway. The study was conducted in accordance with the tenets of the Declaration of Helsinki and was approved by the Regional Committee for Medical and Health Research Ethics (Southern Norway Regional Health Authority). All participants and/or their guardians signed informed consent after full explanation of the study's purpose and procedures.

Clinical Assessment

The participants underwent an eye examination including subjective refraction, slit-lamp biomicroscopy, and color fundus photography (Topcon TRC-NW6S nonmydriatic fundus camera; Topcon Corp., Tokyo, Japan). Monocular visual acuity (logMAR) was measured with a digital high-contrast chart at 6 m (TestChart 2000; Thomson Software Solutions, London, UK). The test distance was reduced to 3 or 1 m if a reliable measurement could not be obtained at the longer distance. Color vision was screened binocularly with the Hardy-Rand-Rittler 4th edition (HRR; Richmond Products, Albuquerque, NM, USA) pseudoisochromatic plates using previously described methods.[28] Those who made two or more errors on red-green (RG) screening plates on the second sitting were tested with the RG diagnostic plates and classified to have mild, medium, or strong RG deficiency depending on errors made on these plates. Those who made one or more errors on the yellow-blue (YB) screening plates on the second sitting were classified as mild, and if errors were made on the YB diagnostic plates, they were classified to have medium or strong YB deficiency depending on errors made on these plates.

The clarity of the lens was evaluated using the Lens Opacities Classification System III (LOCS III).[29] AAK was graded 0 to 3 where stage 0 indicated that the cornea was not affected; stage 1 indicated a partially affected corneal limbus; stage 2 indicated a totally affected limbus, without central corneal involvement; and stage 3 indicated a totally affected limbus with central corneal opacification.[30] ONH was evaluated as present or not based on funduscopy, estimated by the ratio of disc-to-fovea distance and disc diameter (average of horizontal and vertical), and confirmed by measurements on color fundus photographs.[31,32] ONH was defined as present when the ratio was >3.5, meaning that >3.5 optic discs could be apposed between the expected foveal center and the border of the optic disc. Borderline cases were also evaluated based on appearance of the optic disc, and ONH was defined as present if the optic nerve head was obviously small or if the disc showed a typical double ring sign. Glaucoma was noted as present or not based on previous ocular history and treatment.

Foveal Hypoplasia

Foveal hypoplasia was assessed by analyzing structural alterations on spectral domain optical coherence tomography (SD-OCT) images acquired with an OCT2 device (Spectralis; Heidelberg Engineering GmbH, Heidelberg, Germany). Volumetric scans, either $20° \times 20°$ or $30° \times 10°$ (consisting of 49 B-scans and 512–1536 A-scans/B-scan) were centered at the expected foveal center. Between 5 and 20 B-scans (frames) were averaged during acquisition to improve signal-to-noise ratio and compensate for eye motion (TruTrack; Heidelberg Engineering GmbH). Horizontal line scans, with a nominal scan length of 30°, were obtained in eyes where macular volumes could not be obtained. Multiple scans were acquired in the region of the expected foveal location to look for signs of foveal specialization.[21,33,34] The lateral scale of all OCT scans was corrected for individual retinal magnification factor by multiplying the nominal scan length with the ratio between each individual's axial length, obtained with the IOL Master (Carl Zeiss Meditec AG, Jena, Germany), and the OCT default axial length (24 mm).

Horizontal line scans were segmented at the inner limiting membrane (ILM); posterior boundary of the outer plexiform layer (OPL); center of the external limiting membrane (ELM); center of the ellipsoid zone (EZ); center of the interdigitation zone (IZ); and the retinal pigment epithelium-Bruch's Membrane (RPE-BrM) band, using custom software implementing a method similar to that used by Park et al.[35] The foveal center was defined as the section with the minimal foveal thickness (ILM to RPE-BrM) within the foveal depression. When no pit was present, the maximum widening of the outer nuclear layer (OPL to ELM) and/or lengthening of the photoreceptor outer segments (EZ to IZ) was used to identify the expected foveal center. Individual OCT line scans through the foveal center were used to grade foveal hypoplasia in participants with aniridia following the criteria suggested by Thomas et al.[36]: absence of extrusion of plexiform layers (grade 1); grade 1 plus absence of foveal depression (grade 2); grade 2 plus absence of outer segment lengthening (grade 3); and grade 3 plus absence of outer nuclear layer widening (grade 4).

Color Vision

Color vision was examined with a low vision version of the Color Assessment and Diagnosis (CAD-LV) test (City Occupational Ltd., London, UK). The CAD test has been used to examine both congenital[37] and acquired color vision deficiencies,[38,39] and is validated with a reported high test-retest reliability.[40] To ascertain the degree of noncongenital deficiencies and elucidate if it was receptoral or postreceptoral in origin, some participants were invited to do the Cambridge Color Test (CCT; Cambridge Research Systems Ltd., Cambridge, UK), and anomaloscope (HMC Oculus Anomaloscope MR, Type 47700; Oculus Optikgeräte GmbH, Wetzlar, Germany). All participants wore the appropriate refractive correction as determined during the initial clinical assessment.

Color Assessment and Diagnosis Test

The normal controls and 31 of the participants with aniridia were tested with the CAD. The CAD test measures red-green (RG) and yellow-blue (YB) color detection thresholds with a chromatic, moving isoluminant stimulus embedded in a

Investigative Ophthalmology & Visual Science

background of dynamic luminance contrast noise.[41–43] Chromatic thresholds were measured using a 4-alternative-forced-choice method along 16 hue directions in the CIE 1931 (x, y) chromaticity diagram.[44] The test conditions were altered to compensate for low vision (LV) in aniridia—the stimulus was double its default size and moved slower to compensate for reduced visual acuity. That is, the stationary achromatic square array of 15×15 checkers subtended $5.7° \times 5.7°$ in visual angle and the smaller moving chromatic square array of 5×5 checkers subtended $1.8° \times 1.8°$ visual angle at a distance of 140 cm. The temporal frequency was 50% lower than the default setting, and random luminance modulation was increased by 100% to mask the detection of rod-mediated signals that might be introduced by the larger stimulus. Background luminance was 24 cd/m^2. The monitor (SpectraView PA241W; NED Display Solutions, Itasca, IL, USA) was calibrated daily using a photometer (Gossen Mavo Monitor USB, CO Ltd., Nürnberg, Germany).

Median RG and YB thresholds, represented as chromatic difference (CD) from the background chromaticity ($x = 0.305$, $y = 0.323$), were computed.[45] The test was performed binocularly to minimize nystagmus and to indicate overall functional performance, and took 10–12 minutes to complete. As a control, RG and YB thresholds were also measured at a lower luminance level (2.4 cd/m^2; a 1.0 spectrally calibrated neutral density filter was added in front of each eye) for a subset of normal controls ($n = 38$, age 10–67 years).

Cambridge Color Test

The normal controls and 16 of the participants with aniridia (age 11–66 years, logMAR 0.00–0.90) were tested with the CCT Trivector test following standard procedures.[46,47] The test was performed binocularly and took 3 to 4 minutes to complete. Participants were tested twice, and average thresholds were used for analysis. The CCT is a computer-based pseudo-isochromatic test and the stimuli were generated via a graphics system (VSG ViSaGe; Cambridge Research Systems Ltd., Rochester, UK) and presented on a 22-inch CRT monitor (LaCie Electron 22blueIV; LaCie Group, Paris, France). The luminance and chromaticity of the monitor were checked daily with a colorimeter (PR650 Spectra; Photo Research, Inc., Chatsworth, MA, USA). The target was a Landolt-C with inner and outer diameters of 2.2° and 4.3°, respectively, and a gap size of 1° visual angle presented at a test distance of 305 cm. The gap position varied randomly from trial to trial (up, down, left, right), and the observer's task was to indicate the position of the gap by pushing the correct button on a response box within 3 seconds. The test employed a staircase method (11 reversals) for measuring color-discrimination thresholds in three directions along the protan, deutan, and tritan confusion axes in the CIE 1976 (u', v') chromaticity diagram. The maximum color-vector length was set to 0.1600 units. The mean of the last six reversals was taken as the threshold.

Rayleigh Color Match

Ten participants with aniridia performed the Rayleigh color match (Oculus Optikgeräte GmbH) using their best eye. The Rayleigh stimulus is a 2° circular field divided in two semicircles. The upper part is the color-mixture field with a mixture of green (545 nm) and red (671 nm) light, and the lower part is the reference field with yellow light (589 nm). Using the procedure suggested by Linksz,[48] the participant's first task was to find the metameric match between the upper and lower fields by adjusting the luminance of the monochromatic yellow reference field and the relative amounts of red and green light in the mixture field. Theoretically, this is the match that produces the same set of quantum catches at the level of the photoreceptors.[49] This first match was used as the starting point for finding the matching range. Several different relative amounts of red and green light in the mixture field were set by the operator using a staircase procedure, and the participant's task was to judge whether each of them appeared uniform or not by adjusting the luminance of the reference field. The matching range was taken as the difference between the highest and the lowest red/green ratio that the participant would accept after making his/her own luminance adjustments. The mean match midpoint ± SD and matching range for color normal observers for this particular instrument is 40.3 ± 1.91 and 2.01 ± 1.09.[50] A person with a protan deficiency requires more red to match the yellow reference field resulting in a higher than normal match midpoint, whereas someone with a deutan deficiency requires more green resulting in a lower than normal match midpoint. Larger than normal matching ranges signify poorer discrimination, with dichromats accepting all mixture ratios as metameric if the luminance is adjusted appropriately.

Genetic Analysis

All participants, with the exception of participants 5119 and 5124, gave saliva samples (Oragene-DNA, OG-500, DNA Self-Collection Kit; DNA Genotek, Inc., Ottawa, ON, Canada) for genetic analysis of cone opsin gene mutations known to be associated with congenital color vision deficiencies.[24,51] In order to detect genetic evidence of a red-green color vision deficiency, DNA was isolated from saliva samples, and a genotyping performed using a previously described assay.[51] DNA was also used in the PCR to amplify exons 2 through 5 of the L and M opsin genes separately, and exons 2, 3, and 4 were directly sequenced.[28] To identify/confirm the genetic cause of aniridia for each participant, the *PAX6* gene was amplified and sequenced using PCR primers and conditions that were described previously.[52] Fluorescent DNA sequencing was performed on both DNA strands. For participants who were negative for *PAX6* mutations, exons and intron/exon junctions of the *PITX2* and *FOXC1* genes were amplified and sequenced using the PCR primers described by Ansari et al.[53]

Data Analysis

Statistical analysis were performed with R (v3.3.2), R Foundation for Statistical Computing, Vienna, Austria.[54] The data for the aniridia group was found to be nonnormally distributed, as verified by histograms and q-q plots. The nonparametric Mann-Whitney U test was applied for independent samples and the Wilcoxon signed-rank test for paired samples. Correlations were assessed with Spearman correlation coefficients (r_s). Between-group differences were examined with Kruskal-Wallis 1-way ANOVA. The significance level was set to $P \leq 0.05$. Bonferroni-corrected P values are reported for multiple comparisons. Bland-Altman plots were used to compare the CAD and CCT measurements with the nonparametric limits of agreement estimated as the 2.5 and 97.5 quantiles of the differences and the average bias estimated as the median of the differences. The statistical normal limits for the CAD-LV test were computed based on the median color discrimination threshold and the 2.5% quantile and 97.5% quantile (giving a 95% interquantile range) for the normal controls in the study. A quantile regression was conducted to estimate and plot a curve to the median, 2.5% and 97.5% quantiles as a function of age using the quantreg v5.33 package for R.[55] CAD-LV units were calculated to assess the severity of color vision loss in aniridia, dividing the aniridia thresholds by the normal median RG and YB thresholds (based on data from

Investigative Ophthalmology & Visual Science

Table 1. Age Distribution and Number of Participants in Each Age Group

	Aniridia			Normal Controls		
Age Group	*n*	Median Age	Age Range	*n*	Median Age	Age Range
<20	7	12	9–19	11	14	10–19
20–29	9	24	20–29	15	23	20–27
30–49	9	40	31–49	11	41	32–47
50–59	3	51	50–56	5	55	51–58
>60	3	66	64–67	10	67.5	62–74

our 52 controls), respectively. Both thresholds represented as CD $\times 10^4$ and thresholds expressed as CAD-LV units were used for analysis.

Results

Clinical Assessment and Genetics

A total of 31 of 36 participants with aniridia (aged 10–67 years, 12 males) had cone opsin genes known to be associated with normal color vision, including four female carriers of deutan color vision deficiency. Five males with aniridia were excluded from further analysis as they were confirmed to have cone opsin genes conferring congenital deutan color vision deficiency. Table 1 shows the age distribution for all the study participants.

Those with normal opsin genes had corrected visual acuity 0.00 to 1.76 logMAR in their best eye; 11 (35.5%) of these made two or more RG errors on the HRR, four (12.9%) of which also made YB errors, while one (3.2%) made YB errors only. Summary of clinical findings and color vision test results for the participants with aniridia are presented in Tables 2 and 3. The participants who were negative for *PAX6* mutations, were also negative for disease-causing mutations in both the *PITX2* and *FOXC1* genes.

All 52 normal controls had cone opsin genes known to be associated with normal color vision, including five female carriers of deutan color vision deficiency. None of the normal controls made more than one error on the HRR; only two made one error on plate 7 (the most difficult RG screening plate). Their corrected visual acuity was 0.16 logMAR or better in their dominant eye. The controls were healthy with no known systemic disease or ocular abnormalities. Clinical assessment, color fundus photography, and OCT imaging were performed on each participant, and all controls were found to be healthy and free of eye disease. Nuclear opalescence, nuclear color grade, cortical- and posterior subcapsular cataract were graded

Table 2. Summary of Clinical Findings for the Participants With Aniridia*

ID	Age	Genetic Mutation	Visual Acuity,† logMAR	Nystagmus	Aniridia Associated Keratopathy, Grade	Foveal Hypoplasia, Grade	Optic Nerve Hypoplasia	Glaucoma	Lens Status
5124	23	N/A	0.40	N	0	0	N	N	Phakic
5139	15	Unknown	0.00	N	0	0	N	N	Phakic
5132	64	Unknown	0.56	N	0	1	N	Y	Pseudophakic
5134	49	Unknown	0.18	N	1	1	N	N	Pseudophakic
5116	66	*PAX6*	0.40	N	2	2	N	N	Pseudophakic
5120	42	*PAX6*	0.22	N	1	2	N	N	Phakic
5123	24	*PAX6*	0.50	N	2	2	N	N	Phakic
5154	24	Unknown	0.72	Y	1	2	N	N	Phakic
5114	56	*PAX6*	0.86	Y	1	3	Y	Y	Aphakic
5125	15	*PAX6*	0.74	Y	1	3	N	Y	Phakic
5126	12	*PAX6*	0.80	Y	1	3	N	Y	Phakic
5135	40	*PAX6*	0.70	Y	1	3	Y	Y	Phakic
5137	20	*PAX6*	0.70	Y	1	3	N	N	Phakic
5144	32	*PAX6*	0.74	Y	2	3	N	Y	Pseudophakic
5147	11	Unknown	0.50	Y	2	3	N	N	Phakic
5148	49	*PAX6*	0.60	N	2	3	N	Y	Pseudophakic
5113	32	*PAX6*	0.80	Y	2	4	N	N	Phakic
5117	20	Unknown	1.00	Y	2	4	N	Y	Pseudophakic
5119	9	N/A	1.00	Y	1	4	N	Y	Phakic
5127	41	*PAX6*	1.20	Y	2	4	N	Y	Pseudophakic
5131	29	*PAX6*	1.30	Y	1	4	Y	Y	Aphakic
5138	11	*PAX6*	0.90	Y	1	4	N	N	Phakic
5140	19	*PAX6*	0.70	Y	2	4	N	N	Phakic
5141	23	*PAX6*	1.00	Y	2	4	N	N	Phakic
5149	31	*PAX6*	0.90	Y	2	4	N/A	N	Phakic
5110	50	*PAX6*	1.00	Y	3	N/A	Y	Y	Pseudophakic
5118	25	*PAX6*	0.74	Y	3	N/A	N	Y	Pseudophakic
5121	51	*PAX6*	CF	Y	3	N/A	N	N	Phakic
5129	67	*PAX6*	1.30	Y	3	N/A	N	Y	Aphakic
5145	36	*PAX6*	1.76	Y	3	N/A	N/A	N	Pseudophakic
5152	26	Unknown	1.30	Y	3	N/A	N/A	Y	Phakic

CF, counting fingers at 0.5 m; N, no; Y, yes; N/A, not applicable.
* The participants are ordered by the grade of foveal hypoplasia.
† Measured with their best eye.

Investigative Ophthalmology & Visual Science

Table 3. Summary of Color Vision Test Results for the Participants With Aniridia*

		CAD-LV Threshold (CD × 10^4), $n = 27$		CCT, $n = 16$			Rayleigh Match, $n = 10$		HRR, $n = 31$	
ID	Age	RG	YB	Protan	Deutan	Tritan	Midpoint	Range	RG	YB
5124	23	N/A	N/A	–	–	–	–	–	Normal	Normal
5139	15	84	134	50	64	62	–	–	Normal	Normal
5132	64	183	327	296	328	1186	46.2	6.0	Mild	Normal
5134	49	93	193	–	–	–	–	–	Normal	Normal
5116	66	116	170	146	131	133	45.7	4.9	Normal	Normal
5120	42	50	113	84	81	92	41.0	5.1	Normal	Normal
5123	24	118	221	79	86	168	40.2	4.2	Normal	Normal
5154	24	110	167	41	54	72	–	–	Normal	Normal
5114	56	434	1198	320	407	1398	–	–	Medium	Mild
5125	15	196	317	73	74	103	–	–	Normal	Normal
5126	12	94	159	130	121	117	42.6	4.3	Normal	Normal
5135	40	123	187	153	218	286	42.2	6.6	Normal	Normal
5137	20	93	166	136	142	737	44.9	4.0	Normal	Normal
5144	32	104	144	–	–	–	–	–	Normal	Normal
5147	11	143	216	132	128	210	44.4	7.4	Mild	Normal
5148	49	192	497	96	149	1076	44.1	11.4	Mild	Mild
5113	32	154	177	128	120	115	–	–	Mild	Normal
5117	20	186	231	–	–	–	–	–	Normal	Normal
5119	9	N/A	N/A	–	–	–	–	–	Normal	Normal
5127	41	239	210	–	–	–	–	–	Mild	Normal
5131	29	197	154	–	–	–	–	–	Medium	Normal
5138	11	80	141	182	157	192	–	–	Normal	Normal
5140	19	133	213	–	–	–	–	–	Normal	Normal
5141	23	231	238	–	–	–	–	–	Normal	Normal
5149	31	181	277	–	–	–	–	–	Normal	Normal
5110	50	119	213	–	–	–	–	–	Normal	Normal
5118	25	220	848	141	154	739	40.5	7.8	Normal	Mild
5121	51	N/A	N/A	–	–	–	–	–	Mild	Strong
5129	67	621	1292	–	–	–	–	–	Medium	Mild
5145	36	124	196	–	–	–	–	–	Mild	Normal
5152	26	N/A	N/A	–	–	–	–	–	Mild	Normal

N/A, not applicable; RG, red-green; YB, yellow-blue.
* The participants are ordered by the grade of foveal hypoplasia (as in Table 2).

and found to be lower than NO2, NC4, C2, and P0 (LOCS III), respectively. None of the normal controls had undergone cataract surgery.

Color Vision

Figure 1 shows RG and YB CAD-LV thresholds for 27 participants with aniridia (circles) and 52 normal controls (squares) as a function of age. Four participants with aniridia were unable to complete the CAD-LV test, either because of too poor vision ($n = 2$) or of other reasons ($n = 2$; one child and one with cerebral palsy).

RG and YB CAD-LV thresholds for normal controls decreased with increasing age from 10 to 20 years, and YB CAD-LV thresholds increased with increasing age from about 50 years. The median (2.5–97.5% quantile) CAD-LV RG and YB thresholds for the normal controls were 72.7 (45.7–112.4) CD × 10^4 and 163.2 (104.2–256.3) CD × 10^4, respectively. CAD-LV RG and YB thresholds were higher when measured at the mesopic light level (2.4 cd/m^2), with a median (2.5%–97.5% quantile) difference between the two tests of 27.8 (5.3–71.8) and 49.1 (–1.0 to 265.4) CD×10^4, respectively. The median (2.5%–97.5% quantile) thresholds along the protan, deutan and tritan confusion axes for the CCT were 58.5 (31.0–118.6), 56.0 (31.7–99.3) and 83.5 (39.0–257.5) respectively for normal controls.

RG and YB CAD-LV thresholds were significantly higher for those with aniridia compared with age-matched normal controls (Mann-Whitney U test: RG: $P < 0.001$, YB: $P = 0.002$). A total of 19 participants with aniridia had RG thresholds that were higher than the 97.5% quantile that was defined as the upper normal limit based our normal control data, of whom seven also had YB thresholds higher than the 97.5% quantile. None had higher YB threshold than the upper normal limit only. Figure 2 shows CAD-LV YB thresholds as a function of RG thresholds; both calculated as CAD-LV standard units. CAD-LV RG thresholds were significantly higher than the CAD-LV YB thresholds ($Z = 3.1$, $P = 0.001$) in aniridia (Fig. 2).

CCT RG threshold was calculated as the mean of the protan and deutan thresholds. There was good agreement between the CAD-LV and the CCT test, but both RG and YB median CAD-LV were higher than the median CCT thresholds. The median RG difference (CAD-CCT threshold) was 12.2 and 19.7 for normal controls and participants with aniridia, respectively (Fig. 3). The median YB differences in thresholds were 69.5 and 28.9, respectively. However, for three of the participants with aniridia, the CCT tritan thresholds were more than twice as high as their CAD-LV YB threshold.

Ten of those with aniridia agreed to be measured with Rayleigh anomaloscopy. The median matching midpoint was 43.3 (range, 40.2–46.2), with a median matching range of 5.6 (range, 4.0–11.4).

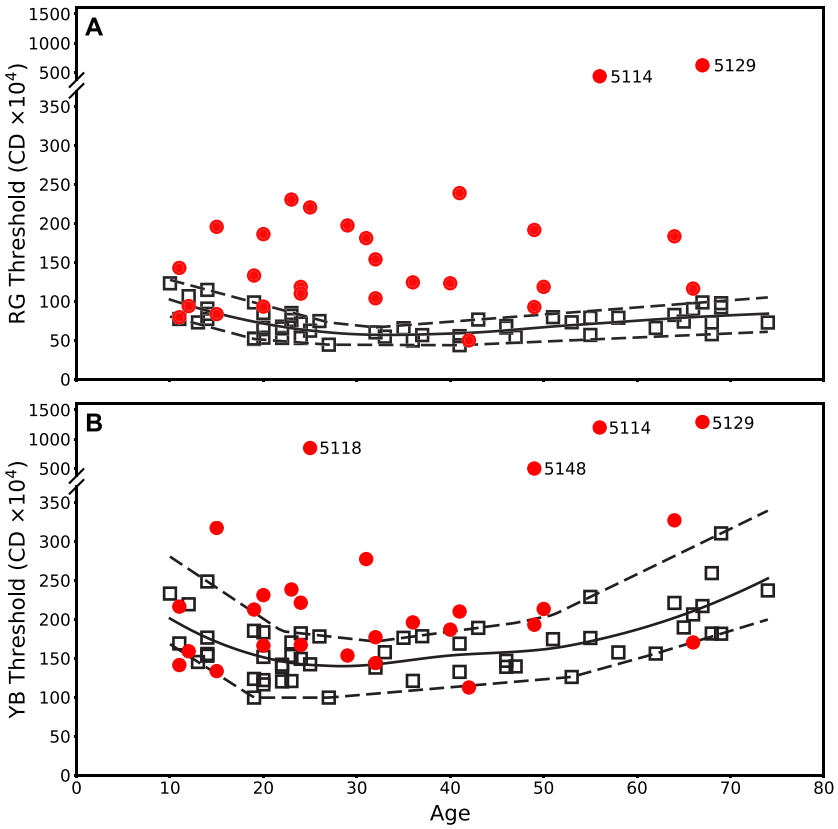

Figure 1. (**A**) CAD-LV RG and (**B**) YB thresholds as a function of age for each observer with aniridia (*filled circles*) and normal controls (*open squares*). The *solid line* shows the fitted median and the *dotted lines* represent the 2.5% and 97.5% quantile estimated with a quantile regression for the normal controls. For clarity, observers with extremely high thresholds (*labeled*) are shown on an extended *y*-axis.

Foveal Hypoplasia and Color Vision in Aniridia

Figure 4 shows OCT scans from five participants with aniridia and foveal hypoplasia grade from 0 to 4. Foveal hypoplasia was observed in 23 of the 25 participants with aniridia imaged with OCT (six had too severe nystagmus and/or ocular media opacities to allow imaging). Two participants had grade 1, four grade 2, eight grade 3 and nine grade 4. One participant had intermediate age-related macular degeneration (which made correct foveal grading difficult) and was, therefore, excluded from the analysis which included structural changes and visual function.

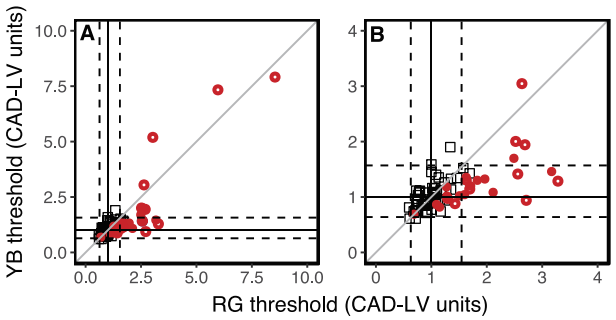

Figure 2. CAD-LV RG and YB threshold for participants with aniridia (*filled circles*), aniridia and secondary glaucoma (*open circles*) and normal controls (*open squares*). Median, 2.5% and 97.5% quantiles for the normal controls are marked. Thresholds are presented in CAD-LV standard units, calculated by dividing the thresholds by the normal median values for RG and YB threshold, respectively. (**A**) All data included, (**B**) Only CV-LV units < 4 units included for better visualization of the individual data points.

There was a strong correlation between the grade of foveal hypoplasia and visual acuity ($r_s = 0.859$, $P < 0.001$). A positive correlation was found between grade of foveal hypoplasia and CAD-LV RG threshold ($r_s = 0.558$, $P = 0.007$), but not for CAD-LV YB threshold ($r_s = 0.255$, $P = 0.252$). Those with foveal hypoplasia grade 0–2 (mild) were grouped and compared with those with grade 3 (moderate) and grade 4 (complete) for between-group comparisons (Fig. 5). Kruskal-Wallis ANOVA revealed a significant difference in CAD-LV RG thresholds between the grades of FH ($\chi^2 = 6.876$, $df = 2$, $P = 0.032$). Those with complete FH (grade 4) had significantly higher CAD-LV RG thresholds than those with mild FH (grade 0–2; $P = 0.038$) (Fig. 5A).

Secondary Pathology and Color Vision in Aniridia

Thirteen of the 27 (48%) participants with aniridia who performed the CAD-LV test had previously been diagnosed with glaucoma and/or ocular hypertension. Six of these had higher than normal thresholds for both CAD-LV RG and YB. Five of these six were also tested on the CCT, and four had higher than normal thresholds for both CCT RG and YB (ID: 5132, 5114, 5148, 5118). The only person without glaucoma who had higher than normal thresholds for both CAD-LV RG and YB (5149) had severe cortical and posterior subcapsular opacification of the lens. The participants with aniridia and the highest thresholds for both CAD-LV RG and YB had either ONH in addition to glaucoma (5114) or high-grade keratopathy in addition to glaucoma (5129, 5118). The other three with ONH had only increased RG threshold.

Kruskal-Wallis ANOVA indicated a difference in CAD-LV YB thresholds between the three AAK severity groups (mild: grade 0–1; moderate: grade 2; severe: grade 3; $\chi^2 = 6.749$, $df = 2$, $P =$

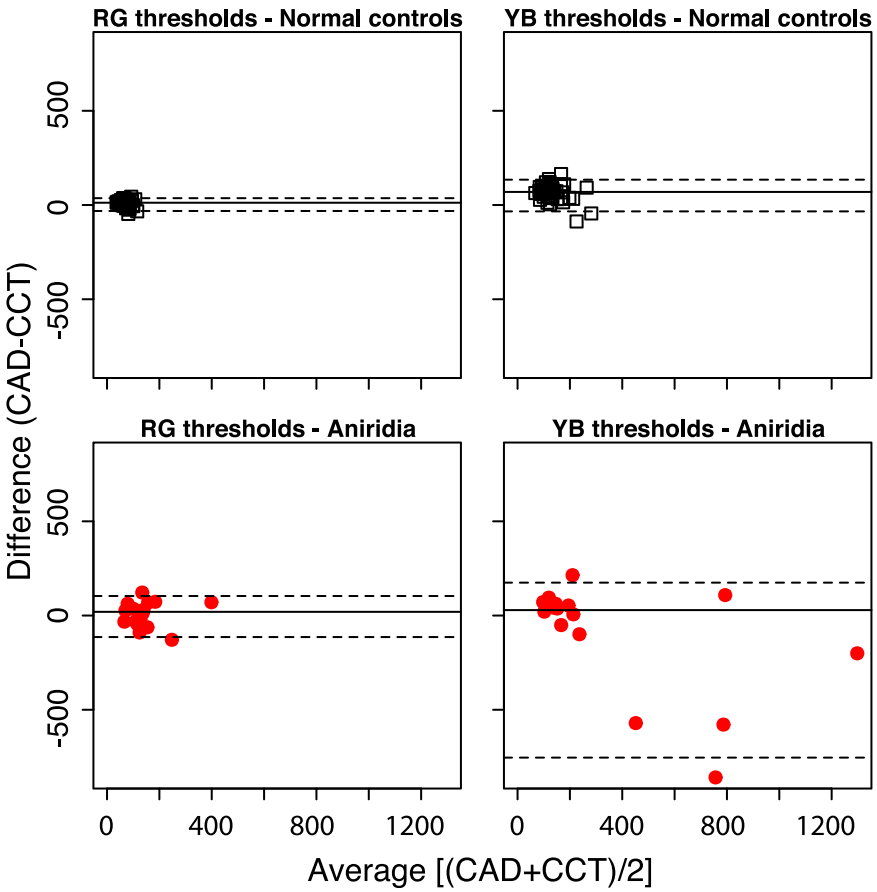

Figure 3. Bland-Altman plots that show the agreement between CAD and CCT. The average [(CAD+CCT/2)] is plotted against the differences (CAD-CCT) for each color discrimination axis for normal controls (*upper row*, *open squares*) and observers with aniridia (*bottom row*, *filled circles*). The *black solid line* represents the median difference, and the *dotted lines* are 2.5% and 97.5% quantiles of the difference.

0.034), but post hoc pairwise comparisons failed to reveal any significant differences (mild/moderate: $P = 0.167$, mild/severe: $P = 0.079$) (Fig. 5D). Note that 12 of 13 with glaucoma also had AAK, and if the 13 with glaucoma were removed from the analysis, only one of the remaining with AAK (5149) had higher than normal CAD-LV YB threshold. The person with glaucoma and no AAK (5132) had higher than normal CAD-LV YB threshold. There were no significant differences in CAD-LV RG thresholds between any of the AAK severity groups (mild/moderate and mild/severe: $P = 0.23$) (Fig. 5C).

Evaluation of lens opacities based on LOCS III grading was only applicable for persons with at least one phakic eye ($n = 18$). Total grading score showed no significant correlation with either RG or YB CAD-LV thresholds ($r_s = 0.296$, $P = 0.305$ and $r_s = 0.252$, $P = 0.384$, respectively).

Discussion

The results presented here show that persons with aniridia exhibit a quantifiable loss of color vision. The greatest loss was in RG color discrimination, which was positively correlated with the grade of foveal hypoplasia. Additional loss was observed in YB color discrimination, but this was associated with secondary ocular pathology, usually glaucoma. Color vision is known to vary as a function of age with maximum sensitivity around 20 years of age, thought to reflect normal healthy development and maturation of the visual system.[56–58] The gradual increase in color discrimination from childhood until early adulthood can be observed for the normal controls in this study, but not for those with aniridia. These findings suggest that a likely reason for loss of red-green color vision in aniridia is arrested foveal formation and associated alterations in retinal structure and processing.

Loss of color vision has been described on one occasion previously, in a family with 11 members with congenital aniridia.[59] We show that loss of RG and YB color vision is frequent in aniridia but cannot always be detected with the HRR pseudoisochromatic plates. Computerized tests, that allow for more accurate measures of chromatic discrimination such as the CAD-LV or the CCT, are required to quantify the loss. General loss in red-green discrimination was also observed for the Rayleigh match, with matching midpoints within normal limits for all except two, but matching ranges more than 2 standard deviations larger than for normal trichromats.[50]

The majority of persons with aniridia ($n = 23$) in this study exhibited the same variation in the degree of foveal hypoplasia (grades 1–4) as previously described for aniridia caused by *PAX6* mutations.[13,36,60] Only two participants had grade 0, both with clearly defined FAZ and RG thresholds within the normal range. Those with complete FH had significantly higher RG thresholds than those with mild FH. There was no association between age, RG thresholds, and FH grade. The degree of FH is most likely associated with the timing of arrested foveal formation,[22,26] resulting in a lower number of L and M cones in the fovea, and foveal cones that are more similar to the peripheral cones with shorter cone outer segments[26] and decreased cone photopigment optical densi-

Investigative Ophthalmology & Visual Science

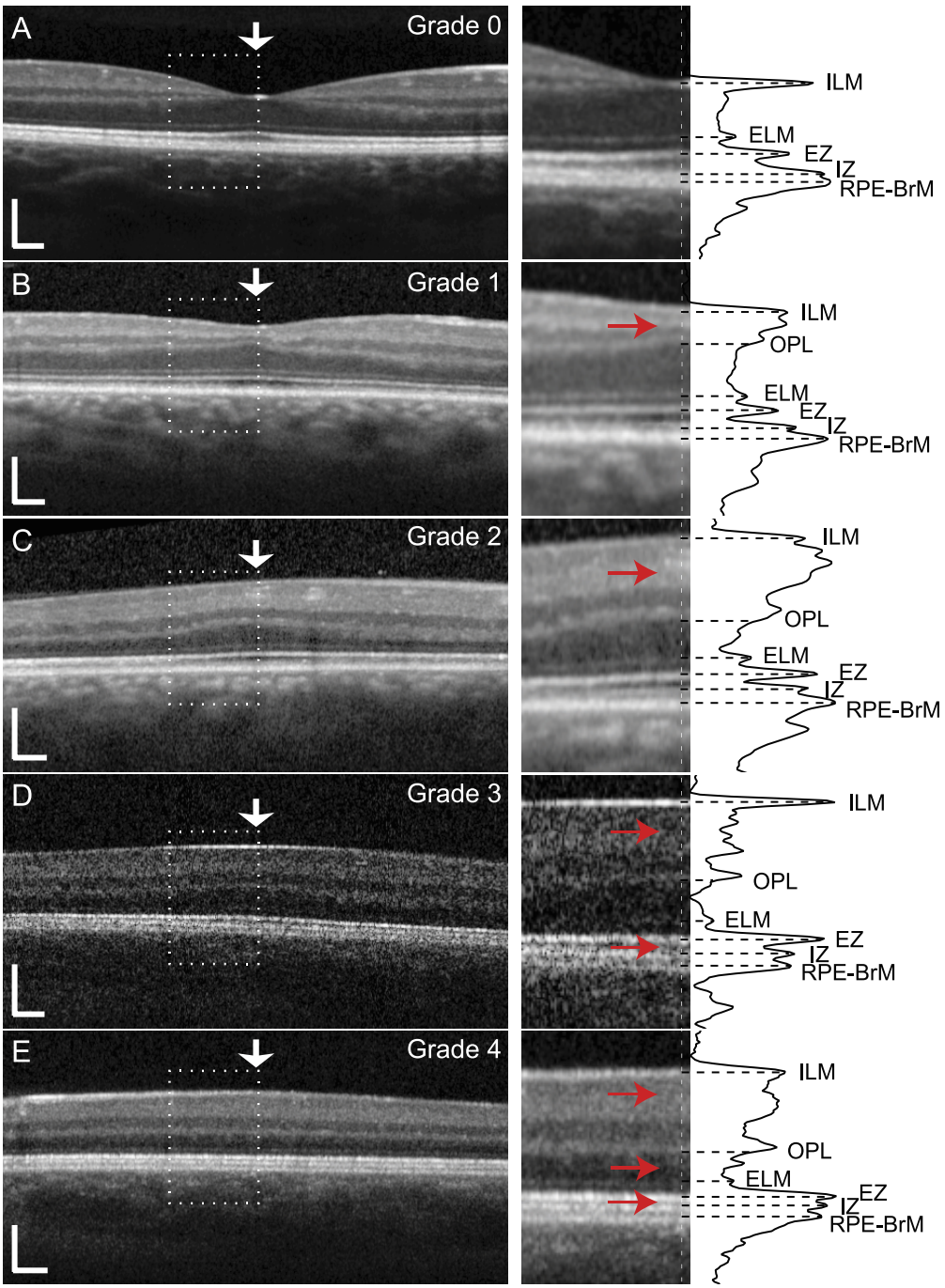

Figure 4. OCT scans from the central 10° of five participants with aniridia (**A–E**) showing the grades (0–4) of foveal hypoplasia.[36] The *dotted rectangle* delineates the ×2 magnified area represented on the right. The marked retinal layers were segmented and analyzed using longitudinal reflectivity profiles averaged over a 5-pixel wide region positioned at the foveal center (*vertical arrows* in *left column*). The distance between the ELM and the posterior boundary of OPL was defined as the outer nuclear layer thickness and the cone outer segments are bounded by the hyperreflective peaks corresponding to IZ and EZ. (**B**) Grade 1 is defined as absence of extrusion of plexiform layers (marked with *arrow* in magnified section on *right*). (**C**) Grade 2 is defined as grade 1 plus absence of foveal depression (marked with *arrow*). (**D**) Grade 3 is defined as grade 2 plus absence of outer segment lengthening (marked with *arrows*). (**E**) Grade 4 is defined as grade 3 plus absence of outer nuclear layer widening (marked with *arrows*). *Scale bars*: 200 μm.

ty.[61] Those who have anirida and associated FH because of *PAX6* mutations may also have a lower ganglion cell density[14,15] and lesser developed cone to midget circuitry (predominance of connections from a single cone to a single midget bipolar cell and a single ganglion cell),[17,19,26] normally located within the FAZ.[20,22] Thus, we argue that altered spatial organization of cone photoreceptors and associated circuitry of the central retina in aniridia is the most likely cause of poorer than normal red-green color discrimination. This is supported by the reduction in cortical volume in the region where the fovea is represented, previously reported in aniridia.[62] We cannot rule out that unstable fixation and

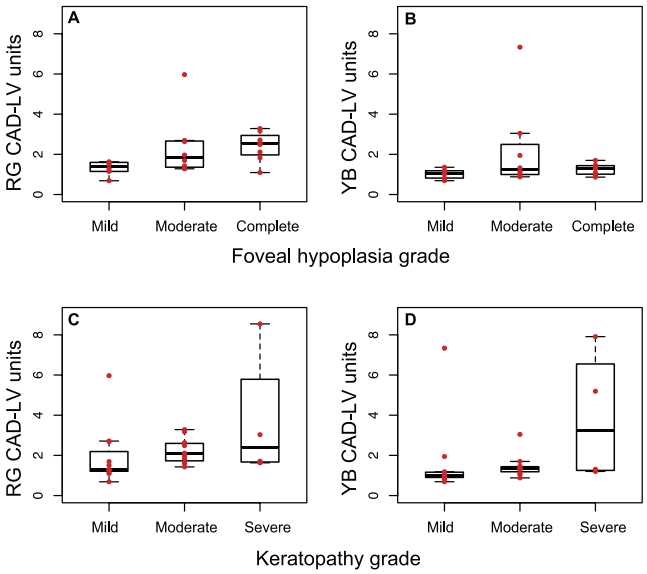

Figure 5. Comparison of CAD-LV RG and YB threshold units between (**A**, **B**) three grades of foveal hypoplasia (mild, grade 0–2; moderate, grade 3; complete, grade 4) and (**C**, **D**) aniridia associated keratopathy. Note that the four participants with severe AAK (**C**, **D**) are not included in any of the FH groups because of insufficient OCT image quality.

nystagmus may also play a role in that a larger part of the retina will be used for sampling a scene, more akin to perifoveal sampling in normal controls.[63,64]

Secondary pathology may aggravate both spatial and color vision function early on in aniridia, because with FH there are most likely far fewer cones and possibly not the same redundancy of cells within the macular region as that observed in normally developed retinas.[65] This is corroborated by previously reported correlations between high contrast achromatic visual acuity and the degree of retinal development as ascertained by the grades of FH.[36] It is known from studies on other retinal degenerative diseases that visual acuity may remain within normal limits even when cone density is less than half of what is observed in normal controls.[66–68]

The RG thresholds were significantly higher than YB thresholds in persons with aniridia, with loss of YB color vision in addition to loss of RG vision appearing to be most strongly associated with glaucoma. Both RG and YB color vision loss have previously been reported in glaucoma,[69–71] with higher thresholds being associated with severity of the disease.[71] The two with aniridia who had the highest RG and YB thresholds, have had glaucoma for more than 20 years (assumed to reflect severity of glaucoma). Loss of YB color vision is also commonly associated with media opacities and a reduction in retinal illuminance caused by increased absorption of short wavelength light.[57,58] There was no significant correlation between YB color vision loss and grade of media opacity here, perhaps because only four participants who performed the CAD test had stage 3 AAK (central corneal involvement), and because of the younger age in the phakic group. The pattern of cataract development in aniridia is also different from typical age-related changes.[6] Combined media opacities (AAK and cataract) in anirida may result in a general reduction of retinal illuminance. But, as measured with an added ND filter (to simulate reduced retinal illuminance) in normal controls, this resulted in an almost uniform increase in both RG and YB CAD-LV thresholds, as opposed to the significantly higher RG thresholds in aniridia.

Both normal and impaired color discrimination has been reported in other disorders associated with foveal hypoplasia,[63,72–75] but it is not known if other pathophysiologic mechanisms that cause FH also affect color discrimination. In aniridia, we surmise that *PAX6* mutation dosage expression is likely to be directly correlated with the degree of FH and the degree of impaired red-green color discrimination. Future work including more detailed *PAX6* genotyping and additional measurement techniques, such as multimodal AOSLO imaging,[76–78] may enable us to test this hypothesis.

Conclusions

In conclusion, visual function loss in aniridia is not limited to loss of visual acuity. Additional loss of color vision appears to be a combined consequence of the timing of arrested foveal formation and secondary ocular pathology. It is a reminder that persons with aniridia are equally likely to inherit congenital color vision deficiencies as others.

Acknowledgments

Supported by the Norwegian Association of Aniridia (Aniridi Norge). The genetic analysis portion of this work was conducted by the University of Washington and was supported by Research to Prevent Blindness, and National Institutes of Health/National Eye Institute Grant P30EY001730. HRP holds a PhD position funded by the Norwegian Ministry of Education and Research.

Disclosure: **H.R. Pedersen**, None; **L.A. Hagen**, None; **E.C.S. Landsend**, None; **S.J. Gilson**, None; **Ø.A. Utheim**, None; **T.P. Utheim**, None; **M. Neitz**, None; **R.C. Baraas**, None

References

1. Edén U, Iggman D, Riise R, Tornqvist K. Epidemiology of aniridia in Sweden and Norway. *Acta Ophthalmol*. 2008;86:727–729.
2. Hingorani M, Williamson KA, Moore AT, van Heyningen V. Detailed ophthalmologic evaluation of 43 individuals with PAX6 mutations. *Invest Ophthalmol Vis Sci*. 2009;50:2581–2590.
3. McCulley TJ, Mayer K, Dahr SS, Simpson J, Holland EJ. Aniridia and optic nerve hypoplasia. *Eye (Lond)*. 2005;19:762–764.
4. Hingorani M, Hanson I, van Heyningen V. Aniridia. *Eur J Hum Genet*. 2012;20:1011–1017.
5. Lee H, Khan R, O'Keefe M. Aniridia: current pathology and management. *Acta Ophthalmol*. 2008;86:708–715.
6. Eden U, Lagali N, Dellby A, et al. Cataract development in Norwegian patients with congenital aniridia. *Acta Ophthalmol*. 2014;92:e165–e167.
7. Netland PA, Scott ML, Boyle JWT, Lauderdale JD. Ocular and systemic findings in a survey of aniridia subjects. *J AAPOS*. 2011;15:562–566.
8. Landsend ES, Utheim OA, Pedersen HR, Lagali N, Baraas RC, Utheim TP. The genetics of congenital aniridia—a guide for the ophthalmologist. *Surv Ophthalmol*. 2018;63:105–113.
9. Vincent MC, Pujo AL, Olivier D, Calvas P. Screening for PAX6 gene mutations is consistent with haploinsufficiency as the main mechanism leading to various ocular defects. *Eur J Hum Genet*. 2003;11:163–169.
10. Shaw MW, Falls HF, Neel JV. Congenital aniridia. *Am J Hum Genet*. 1960;12:389–415.
11. Tzoulaki I, White IM, Hanson IM. PAX6 mutations: genotype-phenotype correlations. *BMC Genet*. 2005;6:27.
12. Holmstrom G, Eriksson U, Hellgren K, Larsson E. Optical coherence tomography is helpful in the diagnosis of foveal hypoplasia. *Acta Ophthalmol*. 2010;88:439–442.

13. Gregory-Evans K, Cheong-Leen R, George SM, et al. Non-invasive anterior segment and posterior segment optical coherence tomography and phenotypic characterization of aniridia. *Can J Ophthalmol*. 2011;46:337–344.
14. Riesenberg AN, Le TT, Willardsen MI, Blackburn DC, Vetter ML, Brown NL. Pax6 regulation of Math5 during mouse retinal neurogenesis. *Genesis*. 2009;47:175–187.
15. Marquardt T, Ashery-Padan R, Andrejewski N, Scardigli R, Guillemot F, Gruss P. Pax6 is required for the multipotent state of retinal progenitor cells. *Cell*. 2001;105:43–55.
16. Schedl A, Ross A, Lee M, et al. Influence of PAX6 gene dosage on development: overexpression causes severe eye abnormalities. *Cell*. 1996;86:71–82.
17. Hsieh YW, Yang XJ. Dynamic Pax6 expression during the neurogenic cell cycle influences proliferation and cell fate choices of retinal progenitors. *Neural Dev*. 2009;4:32.
18. Philips GT, Stair CN, Young Lee H, et al. Precocious retinal neurons: Pax6 controls timing of differentiation and determination of cell type. *Dev Biol*. 2005;279:308–321.
19. Manuel M, Pratt T, Liu M, Jeffery G, Price DJ. Overexpression of Pax6 results in microphthalmia, retinal dysplasia and defective retinal ganglion cell axon guidance. *BMC Dev Biol*. 2008;8:59.
20. Leventhal AG. Evidence that retinal ganglion cell density affects foveal development. *Perspect Dev Neurobiol*. 1996;3:203–211.
21. Yuodelis C, Hendrickson A. A qualitative and quantitative analysis of the human fovea during development. *Vision Res*. 1986;26:847–855.
22. Provis JM, Dubis AM, Maddess T, Carroll J. Adaptation of the central retina for high acuity vision: cones, the fovea and the avascular zone. *Prog Retin Eye Res*. 2013;35:63–81.
23. Hendrickson A, Possin D, Vajzovic L, Toth CA. Histologic development of the human fovea from midgestation to maturity. *Am J Ophthalmol*. 2012;154:767–778.e2.
24. Neitz J, Neitz M. The genetics of normal and defective color vision. *Vision Res*. 2011;51:633–651.
25. Solomon SG, Lennie P. The machinery of colour vision. *Nat Rev Neurosci*. 2007;8:276–286.
26. Xiao M, Hendrickson A. Spatial and temporal expression of short, long/medium, or both opsins in human fetal cones. *J Comp Neurol*. 2000;425:545–559.
27. Cornish EE, Hendrickson AE, Provis JM. Distribution of short-wavelength-sensitive cones in human fetal and postnatal retina: early development of spatial order and density profiles. *Vision Res*. 2004;44:2019–2026.
28. Dees EW, Gilson SJ, Neitz M, Baraas RC. The influence of L-opsin gene polymorphisms and neural ageing on spatio-chromatic contrast sensitivity in 20–71 year olds. *Vision Res*. 2015;116:13–24.
29. Chylack LT Jr, Wolfe JK, Singer DM, et al. The lens opacities classification system III. The longitudinal study of Cataract Study Group. *Arch Ophthalmol*. 1993;111:831–836.
30. Mackman G, Brightbill FS, Optiz JM. Corneal changes in aniridia. *Am J Ophthalmol*. 1979;87:497–502.
31. Barr DB, Weir CR, Purdie AT. An appraisal of the disc-macula distance to disc diameter ratio in the assessment of optic disc size. *Ophthalmic Physiol Opt*. 1999;19:365–375.
32. Sato KI. Reference interval for the disc-macula distance to disc diameter ratio in a large population of healthy Japanese adults: a prospective, observational study. *Medicine (Baltimore)*. 2017;96:e6613.
33. Dubis AM, Costakos DM, Subramaniam CD, et al. Evaluation of normal human foveal development using optical coherence tomography and histologic examination. *Arch Ophthalmol*. 2012;130:1291–1300.
34. Hendrickson AE, Yuodelis C. The morphological development of the human fovea. *Ophthalmology*. 1984;91:603–612.
35. Park JC, Collison FT, Fishman GA, et al. Objective analysis of hyperreflective outer retinal bands imaged by optical coherence tomography in patients with Stargardt disease. *Invest Ophthalmol Vis Sci*. 2015;56:4662–4667.
36. Thomas MG, Kumar A, Mohammad S, et al. Structural grading of foveal hypoplasia using spectral-domain optical coherence tomography a predictor of visual acuity? *Ophthalmology*. 2011;118:1653–1660.
37. Konstantakopoulou E, Rodriguez-Carmona M, Barbur JL. Processing of color signals in female carriers of color vision deficiency. *J Vis*. 2012;12(2):11.
38. O'Neill-Biba M, Sivaprasad S, Rodriguez-Carmona M, Wolf JE, Barbur JL. Loss of chromatic sensitivity in AMD and diabetes: a comparative study. *Ophthalmic Physiol Opt*. 2010;30:705–716.
39. Vemala R, Sivaprasad S, Barbur JL. Detection of early loss of color vision in age-related macular degeneration – with emphasis on drusen and reticular pseudodrusen. *Invest Ophthalmol Vis Sci*. 2017;58:BIO247–BIO254.
40. Seshadri J, Christensen J, Lakshminarayanan V, Bassi CJ. Evaluation of the new web-based "Colour Assessment and Diagnosis" test. *Optom Vis Sci*. 2005;82:882–885.
41. Barbur JL, Rodriguez-Carmona M, Harlow JA, Mancuso K, Neitz J, Neitz M. A study of unusual Rayleigh matches in deutan deficiency. *Vis Neurosci*. 2008;25:507–516.
42. Barbur JL. 'Double-blindsight' revealed through the processing of color and luminance contrast defined motion signals. *Prog Brain Res*. 2004;144:243–259.
43. Barbur JL, Harlow AJ, Plant GT. Insights into the different exploits of colour in the visual cortex. *Proc Biol Sci*. 1994;258:327–334.
44. Rodriguez-Carmona M, Harlow A, Walker G, Barbur J. The variability of normal trichromatic vision and the establishment of the "normal" range. In: Nieves JL, Hernández-Andrés J, eds. *Proceedings of 10th Congress of the International Colour Association*. Granada, Spain: Association Internationale de la Couleur; 2005:979–982.
45. Barbur JL, Rodriguez-Carmona M, Harlow AJ. Establishing the statistical limits of 'normal' chromatic sensitivity. In: *Proceedings of the ISCC/CIE Expert Symposium 2006: 75 Years of the CIE Standard Colorimetric Observer*. Vienna, Austria: International Commission on Illumination; 2006.
46. Regan BC, Reffin JP, Mollon JD. Luminance noise and the rapid determination of discrimination ellipses in colour deficiency. *Vision Res*. 1994;34:1279–1299.
47. Baraas RC, Hagen LA, Dees EW, Neitz M. Substitution of isoleucine for threonine at position 190 of S-opsin causes S-cone-function abnormalities. *Vision Res*. 2012;73:1–9.
48. Linksz A. *An Essay on Color Vision and Clinical Color-Vision Tests*. New York: Grune and Stratton; 1964.
49. Rushton WAH. Review Lecture. Pigments and signals in colour vision. *J Physiol*. 1972;220:1P–31P.
50. Dees EW, Baraas RC. Performance of normal females and carriers of color-vision deficiencies on standard color-vision tests. *J Opt Soc Am A Opt Image Sci Vis*. 2014;31:A401–A409.
51. Davidoff C, Neitz M, Neitz J. Genetic testing as a new standard for clinical diagnosis of color vision deficiencies. *Trans Vis Sci Tech*. 2016;5(5):2.
52. Yokoi T, Nishina S, Fukami M, et al. Genotype-phenotype correlation of PAX6 gene mutations in aniridia. *Hum Genome Var*. 2016;3:15052.
53. Ansari M, Rainger J, Hanson IM, et al. Genetic analysis of 'PAX6-negative' individuals with Aniridia or Gillespie syndrome. *PLoS One*. 2016;11:e0153757.

Investigative Ophthalmology & Visual Science

54. R Core Team. *R: A Language and Environment For Statistical Computing*. Vienna: R Foundation for Statistical Computing; 2016.
55. Koenker R. Quantreg: Quantile Regression. R Package Version 5.33. Available at: https://cran.r-project.org/package=quantreg.
56. Knoblauch K, Vital-Durand F, Barbur JL. Variation of chromatic sensitivity across the life span. *Vision Res*. 2001;41:23–36.
57. Paramei GV, Oakley B. Variation of color discrimination across the life span. *J Opt Soc Am A Opt Image Sci Vis*. 2014;31:A375–A384.
58. Barbur JL, Rodriguez-Carmona M. Color vision changes in normal aging. In: Elliott AJ, Fairchild MD, Franklin A, eds. *Handbook of Color Psychology*. Cambridge, United Kingdom: Cambridge University Press; 2015:180–196.
59. Weber U, Petersen J. Morphological and functional findings in a family with aniridia [in German]. *Klin Monbl Augenheilkd*. 1981;178:439–445.
60. Bredrup C, Knappskog PM, Rodahl E, Boman H. Clinical manifestation of a novel PAX6 mutation Arg128Pro. *Arch Ophthalmol*. 2008;126:428–430.
61. Renner AB, Knau H, Neitz M, Neitz J, Werner JS. Photopigment optical density of the human foveola and a paradoxical senescent increase outside the fovea. *Vis Neurosci*. 2004;21:827–834.
62. Neveu MM, von dem Hagen E, Morland AB, Jeffery G. The fovea regulates symmetrical development of the visual cortex. *J Comp Neurol*. 2008;506:791–800.
63. Lourenço PE, Fishman GA, Anderson RJ. Color vision in albino subjects. *Doc Ophthalmol*. 1983;55:341–350.
64. Hansen T, Pracejus L, Gegenfurtner KR. Color perception in the intermediate periphery of the visual field. *J Vis*. 2009;9(4):26.
65. Dees EW, Dubra A, Baraas RC. Variability in parafoveal cone mosaic in normal trichromatic individuals. *Biomed Opt Express*. 2011;2:1351–1358.
66. Carroll J, Baraas RC, Wagner-Schuman M, et al. Cone photoreceptor mosaic disruption associated with Cys203Arg mutation in the M-cone opsin. *Proc Natl Acad Sci U S A*. 2009;106:20948–20953.
67. Michaelides M, Rha J, Dees EW, et al. Integrity of the cone photoreceptor mosaic in oligocone trichromacy. *Invest Ophthalmol Vis Sci*. 2011;52:4757–4764.
68. Ratnam K, Carroll J, Porco TC, Duncan JL, Roorda A. Relationship between foveal cone structure and clinical measures of visual function in patients with inherited retinal degenerations. *Invest Ophthalmol Vis Sci*. 2013;54:5836–5847.
69. Papaconstantinou D, Georgalas I, Kalantzis G, et al. Acquired color vision and visual field defects in patients with ocular hypertension and early glaucoma. *Clin Ophthalmol*. 2009;3:251–257.
70. Niwa Y, Muraki S, Naito F, Minamikawa T, Ohji M. Evaluation of acquired color vision deficiency in glaucoma using the Rabin cone contrast test. *Invest Ophthalmol Vis Sci*. 2014;55:6686–6690.
71. Rauscher FG, Chisholm CM, Edgar DF, Barbur JL. Assessment of novel binocular colour, motion and contrast tests in glaucoma. *Cell Tissue Res*. 2013;353:297–310.
72. Vincent A, Kemmanu V, Shetty R, Anandula V, Madhavarao B, Shetty B. Variable expressivity of ocular associations of foveal hypoplasia in a family. *Eye (Lond)*. 2009;23:1735–1739.
73. Oliver MD, Dotan SA, Chemke J, Abraham FA. Isolated foveal hypoplasia. *Br J Ophthalmol*. 1987;71:926–930.
74. Grønskov K, Ek J, Brondum-Nielsen K. Oculocutaneous albinism. *Orphanet J Rare Dis*. 2007;2:43.
75. Ilia M, Jeffery G. Retinal cell addition and rod production depend on early stages of ocular melanin synthesis. *J Comp Neurol*. 2000;420:437–444.
76. Scoles D, Sulai YN, Langlo CS, et al. In vivo imaging of human cone photoreceptor inner segments. *Invest Ophthalmol Vis Sci*. 2014;55:4244–4251.
77. Dubra A, Sulai Y. Reflective afocal broadband adaptive optics scanning ophthalmoscope. *Biomed Opt Express*. 2011;2:1757–1768.
78. Pedersen HR, Gilson SJ, Dubra A, Munch IC, Larsen M, Baraas RC. Multimodal imaging of small hard retinal drusen in young healthy adults. *Br J Ophthalmol*. 2018;102:146–152.

Investigative Ophthalmology & Visual Science